

OPEN ACCESS

Role of particle interactions in the Feshbach conversion of fermionic atoms to bosonic molecules

To cite this article: Jie Liu *et al* 2008 *New J. Phys.* **10** 123018

View the [article online](#) for updates and enhancements.

You may also like

- [Recent progresses of ultracold two-electron atoms](#)
Chengdong He, Elnur Hajiyev, Zejian Ren et al.
- [Theoretical analysis of the coupling between Feshbach states and hyperfine excited states in the creation of \$^{23}\text{Na}^{40}\text{K}\$ molecule](#)
Ya-Xiong Liu, , Bo Zhao et al.
- [Efimov physics: a review](#)
Pascal Naidon and Shimpei Endo

Role of particle interactions in the Feshbach conversion of fermionic atoms to bosonic molecules

Jie Liu^{1,2}, Li-Bin Fu², Bin Liu^{3,4} and Biao Wu⁵

¹ Center for Applied Physics and Technology, Peking University, 100084 Beijing, People's Republic of China

² Institute of Applied Physics and Computational Mathematics, Beijing 100088, People's Republic of China

³ Graduate School, China Academy of Engineering Physics, Beijing 100088, People's Republic of China

⁴ College of Physics and Information Engineering, Hebei Normal University, 050016 Shijiazhuang, People's Republic of China

⁵ Institute of Physics, Chinese Academy of Sciences, PO Box 603, Beijing 100190, People's Republic of China

E-mail: Liu.jie@iapcm.ac.cn

New Journal of Physics **10** (2008) 123018 (12pp)

Received 5 August 2008

Published 16 December 2008

Online at <http://www.njp.org/>

doi:10.1088/1367-2630/10/12/123018

Abstract. We investigate the Feshbach conversion of fermionic atom pairs to condensed bosonic molecules with a microscopic model that accounts for the repulsive interactions among all the particles involved. We find that the conversion efficiency is enhanced by the interaction between bosonic molecules, while it is suppressed by the interactions between fermionic atoms and between atoms and molecules. In the adiabatic limit, the combined effect of these interactions can lead to a ceiling of less than 100% on the conversion efficiency for a narrow Feshbach resonance. Our theory agrees with the recent Rice experiment on ⁶Li.

Contents

1. Introduction	2
2. Model	3
3. Main results	6
3.1. Theoretical analysis	6
3.2. Comparison with experiments	9
4. Discussion and conclusion	10
Acknowledgments	11
References	11

1. Introduction

Feshbach resonance has now become a focal point of the research activities in the field of cold atom physics [1]–[4] after its first experimental observation in atomic gases [5]. Among these research activities, the production of diatomic molecules from Fermi atoms with Feshbach resonance is of special interest and has attracted a great deal of attention. Firstly, it is an interesting phenomenon by itself [6]; secondly, it provides unique experimental access to the Bardeen–Cooper–Schrieffer (BCS)–Bose–Einstein condensate (BEC) crossover physics [7]–[9]. So far, by slowly sweeping the magnetic field through the Feshbach resonance, samples of over 10^5 weakly bound molecules at temperatures of a few tens of nanokelvins have been produced from quantum degenerate Fermi gas [10]–[12].

The Feshbach conversion is a complicated process involving many fermionic atoms and bosonic molecules in a sweeping magnetic field that crosses a resonance. The theoretical description of the conversion efficiency as a function of sweep rate, atom mass, atomic density and temperature is still under development. The existing theories include the Landau–Zener (LZ) model of two-body molecular production [13, 14] and its many-body extension at zero temperature [15]–[17], the phase-space density model [18], the equilibration model [19] and the quantum statistics model [20] at finite temperatures.

In the present paper, we study a microscopic model of the Feshbach conversion that accounts for all the two-body interactions, including atom–atom, molecule–molecule and atom–molecule interactions. These interactions are ignored in previous theoretical studies [14]–[17]. We find that these interactions can affect the Feshbach conversion efficiency: the repulsive interaction between molecules tends to enhance the conversion efficiency, whereas the other two repulsive interactions between atoms and between atoms and molecules suppress the efficiency. The role of the particle interactions is more significant for a narrow Feshbach resonance, where, in the adiabatic limit, the combined effect of these interactions can yield a ceiling of less than 100% on the conversion efficiency. This interaction-suppressed conversion efficiency is in spirit the same as the broken adiabaticity by interaction in nonlinear LZ tunneling [21, 22]. Our theory has been compared with experiments and is in good agreement with experimental results on ^6Li [11] for the whole range of sweeping rates.

2. Model

To include all particle interactions, we extend the two-channel model in [20], [23]–[25] and write the Hamiltonian as

$$\begin{aligned}
 H = & \sum_{\mathbf{k},\sigma} \epsilon_{\mathbf{k}} a_{\mathbf{k},\sigma}^{\dagger} a_{\mathbf{k},\sigma} + \left(\gamma + \frac{\epsilon_b}{2} \right) b^{\dagger} b \\
 & + \frac{U_a}{V_a} \sum_{\mathbf{k},\mathbf{k}'} a_{\mathbf{k},\uparrow}^{\dagger} a_{-\mathbf{k},\downarrow}^{\dagger} a_{-\mathbf{k}',\downarrow} a_{\mathbf{k}',\uparrow} \\
 & + \frac{U_{ab}}{V_a} \sum_{\mathbf{k},\sigma} a_{\mathbf{k},\sigma}^{\dagger} a_{\mathbf{k},\sigma} b^{\dagger} b + \frac{U_b}{V_b} b^{\dagger} b^{\dagger} b b \\
 & + \frac{g V_b}{V_a^{3/2}} \sum_{\mathbf{k}} \left(b^{\dagger} a_{-\mathbf{k},\downarrow} a_{\mathbf{k},\uparrow} + a_{\mathbf{k},\uparrow}^{\dagger} a_{-\mathbf{k},\downarrow}^{\dagger} b \right). \tag{1}
 \end{aligned}$$

Here, $\epsilon_{\mathbf{k}} = \hbar^2 k^2 / 2m_a$ is the kinetic energy of the atom, $\sigma = \uparrow, \downarrow$ denotes the two hyperfine states of the atom, and $\epsilon_b/2$ is the molecular energy. $U_b = 4\pi \hbar^2 a_{bb} / m_b$ is the interaction between molecules. Other parameters are associated with atoms and are renormalized. With the renormalization factor Λ , these parameters are related to a set of bare parameters, U_0 , U_1 , g_0 and γ_0 , via the standard renormalization relations [3],

$$U_a = \Lambda U_0, \quad U_{ab} = \Lambda U_1, \tag{2}$$

$$g = \Lambda g_0, \quad \gamma = \gamma_0 - (\Lambda g_0^2 / U_c). \tag{3}$$

The renormalization factor is given by

$$\Lambda \equiv (1 + (U_0 / U_c))^{-1}, \quad U_c^{-1} = - \sum_{\mathbf{k}} \frac{\exp(-k^2 / k_c^2)}{2\epsilon_{\mathbf{k}}} \tag{4}$$

with the cutoff momentum k_c representing the inverse range of interactions [25]–[27]. The bare parameters are

$$\gamma_0 = \mu_{co} (B - B_0), \quad g_0 = \sqrt{\frac{4\pi \hbar^2 a_{bg} \Delta B \mu_{co}}{m_a}}, \tag{5}$$

$$U_0 = \frac{4\pi \hbar^2 a_{bg}}{m_a}, \quad U_1 = \frac{4\pi \hbar^2 a_{ab}}{m_{ab}}. \tag{6}$$

In the above, B is the applied magnetic field, which changes linearly with time at a rate of α_r , i.e., $B = -\alpha_r t$ in our study. B_0 and ΔB are the position and width, respectively, of the Feshbach resonance. m_a and $m_b = 2m_a$ are the masses of the atoms and molecules, and $m_{ab} = \frac{2}{3}m_a$ is the reduced mass of the atom–molecule interaction. In addition, μ_{co} is the difference in magnetic moment between the two channels, and we have assumed that the s-wave scattering length near resonance has the form $a_s = a_{bg} (1 - (\Delta B / (B - B_0)))$ with a_{bg} being the background atomic scattering length. The scattering length of atom–molecule and molecule–molecule interactions is denoted by a_{ab} and a_{bb} , respectively.

Due to the trapping potential in experiments, the molecular bosons are more tightly confined in space than the fermionic atoms due to their different statistics [28]. To show this,

we use V_a for the volume of fermionic atoms and V_b for bosonic molecules. We assume the zero-temperature limit, where we can consider only one bosonic mode and ignore all possible dissipations in the system, such as the loss of atoms by three-body collisions.

Due to the presence of an external magnetic field, the ‘spin-up’ and ‘spin-down’ states actually have a Zeeman component (h) to their energy, i.e. $\epsilon_{\mathbf{k}\uparrow} = \epsilon_{\mathbf{k}} + h$, $\epsilon_{\mathbf{k}\downarrow} = \epsilon_{\mathbf{k}} - h$. However, the total energy of the non-interacting atoms $\sum_{\mathbf{k},\sigma} \epsilon_{\mathbf{k},\sigma} a_{\mathbf{k},\sigma}^\dagger a_{\mathbf{k},\sigma}$ can be rewritten as

$$\sum_{\mathbf{k}} \left[\epsilon_{\mathbf{k}} (a_{\mathbf{k}\uparrow}^\dagger a_{\mathbf{k}\uparrow} + a_{\mathbf{k}\downarrow}^\dagger a_{\mathbf{k}\downarrow}) + h (a_{\mathbf{k}\uparrow}^\dagger a_{\mathbf{k}\uparrow} - a_{\mathbf{k}\downarrow}^\dagger a_{\mathbf{k}\downarrow}) \right]. \quad (7)$$

In our study, the numbers of ‘spin-up’ atoms and ‘spin-down’ atoms are the same. Therefore, the second term in the above expression vanishes, and we have not written down the Zeeman energy term in equation (1).

In the current experiments, the intrinsic energy width of a Feshbach resonance is larger than the Fermi energy E_F [29]; it is therefore reasonable to assume $\epsilon_{\mathbf{k}} = \epsilon$. This approximation is called the degenerate model in [15, 16, 24] and has been verified by exact numerical calculations in [15, 16]. In the present study, we will use this degenerate approximation.

We proceed by introducing the following operators [15, 16]:

$$L_x = \frac{\sum_{\mathbf{k}} (a_{\mathbf{k}\uparrow}^\dagger a_{-\mathbf{k}\downarrow}^\dagger b + b^\dagger a_{-\mathbf{k}\downarrow} a_{\mathbf{k}\uparrow})}{(N/2)^{3/2}}, \quad (8)$$

$$L_y = \frac{\sum_{\mathbf{k}} (a_{\mathbf{k}\uparrow}^\dagger a_{-\mathbf{k}\downarrow}^\dagger b - b^\dagger a_{-\mathbf{k}\downarrow} a_{\mathbf{k}\uparrow})}{i(N/2)^{3/2}}, \quad (9)$$

$$L_z = \frac{\sum_{\mathbf{k},\sigma} a_{\mathbf{k},\sigma}^\dagger a_{\mathbf{k},\sigma} - 2b^\dagger b}{N}, \quad (10)$$

where $N = 2b^\dagger b + \sum_{\mathbf{k},\sigma} a_{\mathbf{k},\sigma}^\dagger a_{\mathbf{k},\sigma}$ is the total number of atoms. The Hamiltonian in equation (1) becomes⁶

$$\begin{aligned} H = & \frac{N}{4} \left[2\epsilon - \left(\gamma + \frac{\epsilon_b}{2} \right) - \frac{NU_a}{2V_a} - \frac{NU_{ab}}{V_a} \right] L_z \\ & - \frac{N^2}{16} \left(\frac{U_a}{V_a} + \frac{2U_{ab}}{V_a} - \frac{U_b}{V_b} \right) (1 - L_z)^2 \\ & + \frac{gV_b}{V_a^{3/2}} \left(\frac{N}{2} \right)^{3/2} L_x. \end{aligned} \quad (11)$$

With the commutators

$$[L_z, L_x] = \frac{4i}{N} L_y, \quad [L_z, L_y] = -\frac{4i}{N} L_x, \quad (12)$$

$$[L_x, L_y] = \frac{i}{N} (1 - L_z)(1 + 3L_z) + O\left(\frac{1}{N^2}\right), \quad (13)$$

⁶ In deducing the atom–atom scattering term, we need to introduce the collective pseudo-spin operators $\hat{S}^+ = \sum_{\mathbf{k}} a_{\mathbf{k}\uparrow}^\dagger a_{-\mathbf{k}\downarrow}^\dagger$, $\hat{S}^- = \sum_{\mathbf{k}} a_{-\mathbf{k}\downarrow} a_{\mathbf{k}\uparrow}$ and $\hat{S}_z = \sum_{\mathbf{k}} \frac{1}{2} (a_{\mathbf{k}\uparrow}^\dagger a_{\mathbf{k}\uparrow} + a_{-\mathbf{k}\downarrow}^\dagger a_{-\mathbf{k}\downarrow} - 1)$. It is easy to prove that $\hat{S}^2 = \hat{S}_z^2 - \hat{S}_z + \hat{S}^+ \hat{S}^-$ is a conservation and $S = N/4$. Combining the conserved relation of the total particles, $N/4 = \hat{b}^\dagger \hat{b} + \hat{S}_z$, we can rewrite the atom–atom scattering term as $\hat{S}^+ \hat{S}^- = \frac{1}{2} \sum_{\mathbf{k},\sigma} a_{\mathbf{k},\sigma}^\dagger a_{\mathbf{k},\sigma} \hat{b}^\dagger \hat{b} + (N/2) - \hat{b}^\dagger \hat{b}$.

we obtain the Heisenberg equations for the system

$$\begin{aligned} \hbar \frac{dL_x}{dt} = & - \left[2\epsilon - \left(\gamma + \frac{\epsilon_b}{2} \right) - \frac{NU_a}{2V_a} - \frac{NU_{ab}}{V_a} \right] L_y \\ & - \frac{N}{4} \left(\frac{U_a}{V_a} + \frac{2U_{ab}}{V_a} - \frac{U_b}{V_b} \right) [(1 - L_z)L_y + L_y(1 - L_z)], \end{aligned} \quad (14)$$

$$\begin{aligned} \hbar \frac{dL_y}{dt} = & \left[2\epsilon - \left(\gamma + \frac{\epsilon_b}{2} \right) - \frac{NU_a}{2V_a} - \frac{NU_{ab}}{V_a} \right] L_x \\ & + \frac{N}{4} \left(\frac{U_a}{V_a} + \frac{2U_{ab}}{V_a} - \frac{U_b}{V_b} \right) [(1 - L_z)L_x + L_x(1 - L_z)] \\ & - \frac{\sqrt{2}gV_b\sqrt{N}}{4V_a^{3/2}} (1 - L_z)(1 + 3L_z) + O\left(\frac{1}{\sqrt{N}}\right), \end{aligned} \quad (15)$$

$$\hbar \frac{dL_z}{dt} = \frac{\sqrt{2}gV_b\sqrt{N}}{V_a^{3/2}} L_y. \quad (16)$$

In the mean-field approximation, we need to replace the operators in the above equations with their expectations, such as using $\langle L_x \rangle$ for L_x . However, these equations show that the expectation values of the single operators, e.g. $\langle L_x \rangle$, depend not only on themselves, but also on the second-order moments, e.g. $\langle L_x L_y \rangle$. Similarly, the time evolution of the second-order moments depends on the third-order moments, and so on. Consequently, we obtain a hierarchy of equations of motion for the expectation values. In order to obtain a closed set of equations of motion, the hierarchy must be truncated at some stage by approximating the N th order moments in terms of lower-order moments [16, 30]. The lowest-order truncation is achieved by approximating the second-order moments with the products of the expectation values of the corresponding single operators, such as $\langle L_x L_y \rangle$ with $\langle L_x \rangle \cdot \langle L_y \rangle$. This truncation is further justified by the following fact. In our study, the total number of atoms N is large. We notice that the commutators in equations (12) and (13) vanish and L_x , L_y and L_z commute with each other, in the limit of large N . In this case, one usually expects factorization relations such as $\langle L_x L_y \rangle = \langle L_x \rangle \cdot \langle L_y \rangle$ [31].

With the introduction of three real numbers u , v and w for the expectation values of the three operators L_x , L_y and L_z and ignoring the $O(1/\sqrt{N})$ term, the above Heisenberg equations become a set of mean-field equations,

$$\frac{du}{d\tau} = -\delta v - 2\chi v(1 - w), \quad \frac{dw}{d\tau} = \sqrt{2}v, \quad (17)$$

$$\frac{dv}{d\tau} = \frac{3\sqrt{2}}{4}(w - 1) \left(w + \frac{1}{3} \right) + \delta u + 2\chi u(1 - w), \quad (18)$$

where

$$\begin{aligned} \tau = & \frac{gV_b\sqrt{N}}{\hbar V_a^{3/2}} t, \\ \delta = & \left[2\epsilon - \left(\gamma + \frac{\epsilon_b}{2} \right) - \frac{NU_a}{2V_a} - \frac{NU_{ab}}{V_a} \right] \frac{V_a^{3/2}}{gV_b\sqrt{N}}, \\ \chi = & \left(U_a + 2U_{ab} - \frac{U_b V_a}{V_b} \right) \frac{\sqrt{N}V_a}{4gV_b}. \end{aligned} \quad (19)$$

Because of the identity $u^2 + v^2 = \frac{1}{2}(w-1)^2(w+1)$, there are only two independent variables. By introducing the variable $\theta = \arctan(v/u)$, which is canonically conjugate to w , we have a classical Hamiltonian,

$$\mathcal{H} = \delta w - \chi(1-w)^2 + \sqrt{(w-1)^2(w+1)} \cos \theta. \quad (20)$$

The above equations show that all the experimental parameters affect the system via only two dimensionless parameters, δ and χ . By a trivial shift of the time origin, we can set $\delta = \alpha\tau$ with

$$\frac{\alpha_r}{\alpha} = \frac{4\pi\hbar n a_{\text{bg}} \Delta B}{m_a} \Lambda^2 \frac{V_b^2}{V_a^2}, \quad (21)$$

where $n = N/V_a$ is the mean atomic density, α is the scaled sweeping rate, and τ is the scaled time. The nonlinear parameter χ is given by

$$\chi = \frac{1}{2} \left(1 + \frac{3a_{\text{ab}}}{a_{\text{bg}}} - \frac{a_{\text{bb}} V_a}{2a_{\text{bg}} \Lambda V_b} \right) \frac{V_a}{V_b} \sqrt{\frac{\pi \hbar^2 a_{\text{bg}} n}{m_a \mu_{\text{co}} \Delta B}}. \quad (22)$$

The Hamiltonian (20) has the energy unit of $\frac{4V_a^{3/2}}{gV_b N^{3/2}}$. The variable w measures the imbalance between atom pairs and molecules and varies in the range of $[-1, 1]$ with $w = -1$ corresponding to a pure molecular gas and $w = 1$ to a pure atomic gas. We are interested in how many atomic pairs are converted to molecules after the magnetic field crosses the resonance. We use w_f to denote the value of w long after the magnetic field has passed the resonance. The molecular conversion efficiency is defined as $T = 1 - \Gamma = \frac{1-w_f}{2}$, while the fraction of unconverted atoms is defined as $\Gamma = \frac{1+w_f}{2}$.

3. Main results

3.1. Theoretical analysis

To understand the dynamics of the Hamiltonian (20), we first look at the fixed points of this system. They can be found by setting $\dot{w} = \dot{\theta} = \dot{v} = 0$ in equations (17) and (18). The energies for these fixed points make up energy levels of the system as shown in figure 1. One can see that the structure of these energy levels changes dramatically as the nonlinear parameter χ increases. Specifically, we observe the following. (i) There are two fixed points P_1 and P_2 when $|\delta|$ is large enough: one for the bosonic molecule (BM) and the other for the fermionic atom (FA). (ii) When $|\delta| < \delta_c = \sqrt{2}$, there is an additional fixed point with $w = 1$, which is represented by MQ in figure 1. However, this fixed point is dynamically unstable [22]. (iii) For $\chi > \chi_c = \sqrt{2}/4$, there appears one more fixed point denoted by P_3 and, consequently, a loop in the energy levels. As we shall see, this loop has highly nontrivial physical consequences. The fixed point P_3 is also unstable.

Consider the adiabatic evolution of the system starting from a high negative value of δ with $w = 1$. This corresponds to the experiments where the magnetic field sweeps slowly across the Feshbach resonance with initially no bosonic molecules. When χ is small, as in figure 1(a), the evolution of the system follows the solid line, converting all fermionic atoms into molecules. However, when χ is beyond χ_c , as in figure 1(c), the system will find no stable energy level to follow at a single point M . As a result, only a fraction of fermionic atoms are converted into bosonic molecules.

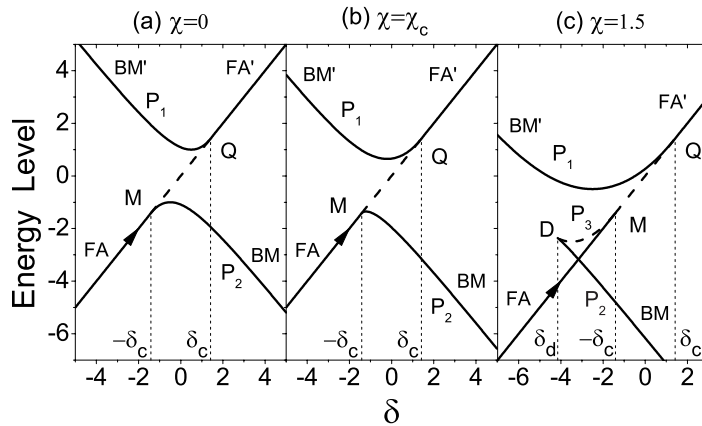


Figure 1. Adiabatic energy levels for different interaction strengths. (a) $\chi = 0$; (b) $\chi = \chi_c = \sqrt{2}/4$; (c) $\chi = 1.5$. The unstable states are indicated by dashed lines (MQ and DM).

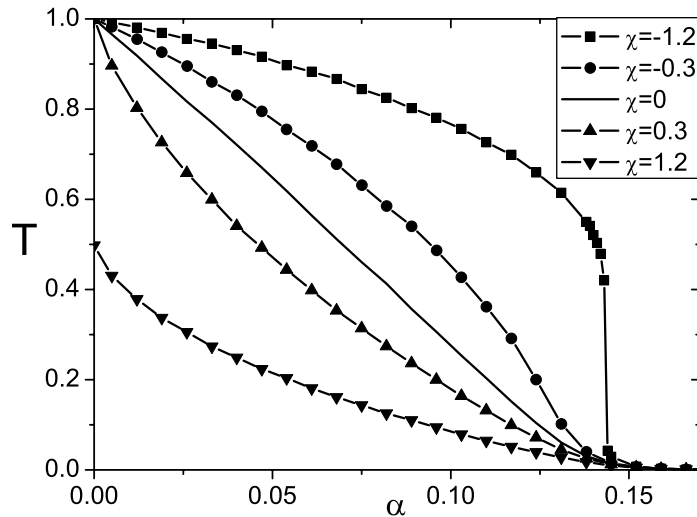


Figure 2. The conversion efficiency T as a function of the sweeping rate α for various interactions.

This simple analysis is confirmed by our numerical results, which are plotted in figure 2. In our calculations, the fourth to fifth Runge–Kutta step-adaptive algorithm is used for solving the differential equations (17) and (18). Because $w = 1$ is a fixed point when $\delta < -\sqrt{2}$, we start from $(w, u, v) \approx (1, 0, 0)$ and sweep the field from $\delta = -\sqrt{2}$ to 200. Then w_f is recorded and the conversion efficiency T is obtained by using the relation $T = \frac{1-w_f}{2}$. In figure 2, the conversion efficiency T , i.e. the fraction of the converted fermionic atom pairs, is drawn as a function of α . Evidently, T approaches 1 as $\alpha \rightarrow 0$ when $\chi < \chi_c$, indicating that all atomic pairs are converted into molecules. In contrast, when $\chi > \chi_c$, T does not increase to 1 in the adiabatic limit $\alpha \rightarrow 0$. This means that there is a ceiling T_{ad} ($< 100\%$) on the conversion efficiency. Moreover, figure 2 demonstrates that positive χ suppresses the conversion efficiency, whereas negative χ enhances it. Because the repulsive interaction between bosonic molecules enters χ as a negative value, it

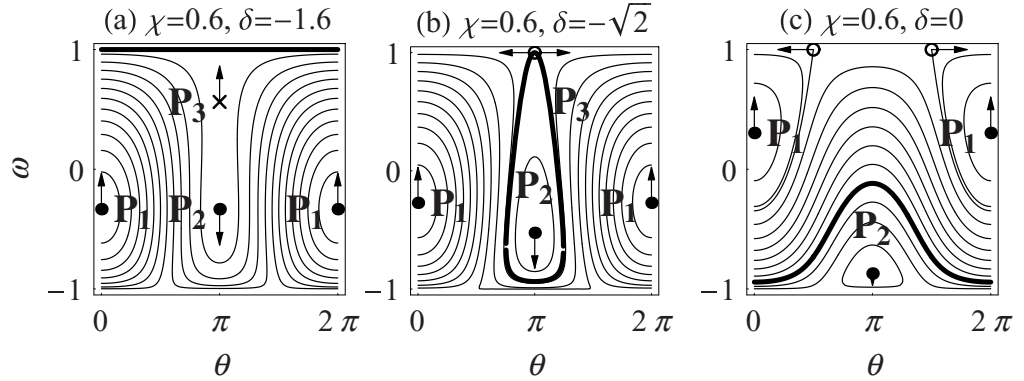


Figure 3. Phase spaces of the Hamiltonian (20). The dark line in (a) is for the fixed point $w = 1, u = 0, v = 0$. It is a line because θ is not defined at $u = v = 0$. The two fixed points on line $w = 1$ in (c) are in fact the same fixed point; they are an artefact caused by the definition $\theta = \arctan(v/u)$.

enhances the conversion efficiency; the repulsive fermionic atom interaction and atom–molecule interaction contribute positively to χ , so they suppress the conversion.

The ceiling T_{ad} on the atom–molecule conversion efficiency depends on χ . This dependence can be found by examining the phase-space diagrams of our system shown in figure 3. As δ ramps up slowly from a large negative value, the fixed point P_3 will move up until it hits the fixed point $w = 1, u = 0, v = 0$, represented by a dark straight line in figure 3(a). This collision occurs at $\delta = -\sqrt{2}$. Immediately after the collision, the hyperbolic fixed point P_3 is no longer a fixed point and becomes a solution that evolves along the dark line in figure 3(b). The dark line is given by $\sqrt{2} = \chi(1 - w) - \sqrt{1 + w} \cos \theta$, which is found by taking $E = \delta = -\sqrt{2}$ in the Hamiltonian (20). As the action of this trajectory is nonzero, whereas a fixed point has zero action, this collision of the two fixed points represents a sudden jump in action. It is this sudden jump that has caused the nonzero fraction of remnant atoms. As δ ramps up further slowly, the trajectory will change its shape as witnessed in figure 3(c); however, its action stays constant as demanded by the classical adiabatic theorem [32, 33]. The action is

$$I = \begin{cases} \frac{1}{2\pi} \oint \frac{\cos \theta \sqrt{8\chi^2 - 4\sqrt{2}\chi + \cos^2 \theta}}{2\chi^2} d\theta, & \frac{\sqrt{2}}{4} < \chi < \frac{\sqrt{2}}{2}; \\ \frac{1}{2\pi} \int_0^{2\pi} \frac{4\chi^2 - 2\sqrt{2}\chi + \cos^2 \theta}{2\chi^2} d\theta, & \chi > \frac{\sqrt{2}}{2}. \end{cases} \quad (23)$$

According to the definition of the action, we have the relation $I = w_f + 1$. Using the relation between the conversion efficiency and the variable w_f , we obtain a ceiling on the efficiency in the adiabatic limit,

$$T_{\text{ad}} = \begin{cases} \frac{4\sqrt{2}\chi - 1}{8\chi^2}, & \chi > \frac{\sqrt{2}}{4}; \\ 1, & \chi < \frac{\sqrt{2}}{4}. \end{cases} \quad (24)$$

3.2. Comparison with experiments

Now we compare our theory with the existing experiments. For the experiment with ${}^6\text{Li}$ [11], the mean density is $n = 4 \times 10^{12} \text{ cm}^{-3}$ with $N = 6 \times 10^5$ atoms. The scattering length is $a_{\text{bg}} = 59a_{\text{B}}$ and the magnetic moment difference is $\mu_{\text{co}} \sim 2\mu_{\text{B}}$, where a_{B} and μ_{B} are the Bohr radius and the Bohr magneton, respectively. The Feshbach resonance is at $B_0 = 543.8 \text{ G}$ with a width of $\Delta B = 0.1 \text{ G}$. The Fermi energy E_{F} in the combined harmonic and box-like trapping potential of [11] is given by $E_{\text{F}} = [15\pi N \hbar^3 \omega_{\text{r}}^2 / (8\sqrt{2m_{\text{a}}L})]^{2/5}$, where $\omega_{\text{r}} = 2\pi \times 800 \text{ s}^{-1}$ is the angular frequency of the radial harmonic trap and $L = 480 \mu\text{m}$ is the size of the axial potential. The ground-state energy of molecular bosons is $E_{\text{G}} = \hbar\omega_{\text{r}} + \hbar^2\pi^2 / (2m_{\text{b}}L^2)$. In the axial (z) direction, the distribution of the cold particles is extended over the whole box of length L and is independent of particle energy, whereas in the radial direction of the harmonic trap ($r = \sqrt{x^2 + y^2}$), the spatial extension of particles is proportional to the square root of their energy. Because bosonic molecules populate only the ground state while fermionic atoms have an energy distribution of up to E_{F} , our estimation shows that the ratio between spatial confinement of bosonic molecules and fermionic atoms is $V_{\text{a}}/V_{\text{b}} = E_{\text{F}}/E_{\text{G}} = 36$. We set $\Lambda = 391$ with a momentum cutoff $K_{\text{c}} = 96k_{\text{F}}$ ⁷. According to equation (21), the sweeping rate is $\alpha_{\text{r}}/\alpha = 20 \text{ G ms}^{-1}$.

The scattering lengths of atom–molecule and molecule–molecule interactions are related to the atom–atom scattering length as $a_{\text{ab}} \approx 1.2a_{\text{bg}}$ and $a_{\text{bb}} \approx 0.6a_{\text{bg}}$ [34, 35]. Substituting these two relations into equation (22), we obtain an explicit expression for the nonlinear parameter,

$$\chi = \left(2.3 - \frac{0.15V_{\text{a}}}{\Lambda V_{\text{b}}} \right) \frac{V_{\text{a}}}{V_{\text{b}}} \sqrt{\frac{\pi \hbar^2 a_{\text{bg}} n}{m_{\text{a}} \mu_{\text{co}} \Delta B}}. \quad (25)$$

The second term in the above parentheses accounts for the repulsive interaction between bosonic molecules and is small. So, the above expression can be approximately reduced to

$$\chi \simeq 2.3 \frac{V_{\text{a}}}{V_{\text{b}}} \sqrt{\frac{\pi \hbar^2 a_{\text{bg}} n}{m_{\text{a}} \mu_{\text{co}} \Delta B}}. \quad (26)$$

For the experimental parameters of ${}^6\text{Li}$, the interaction parameter is $\chi = 1.26$. This strong interaction ($> \chi_{\text{c}}$) leads to a ceiling of $T_{\text{ad}} = 0.48$ via equation (24). This is in good agreement with experiments (see figure 4(a)).

For ${}^{40}\text{K}$, the Feshbach resonance at $B_0 = 202.1 \text{ G}$ has a large width of $\Delta B = 7.8 \text{ G}$ and the mass of ${}^{40}\text{K}$ is 7 times that of ${}^6\text{Li}$. In [18], the fermions are confined in a dipole trap characterized by a radial frequency ν_{r} between 312 and 630 Hz, i.e. an aspect ratio of $\nu_{\text{r}}/\nu_{\text{z}} = 70$. The Fermi energy is $E_{\text{F}} = \hbar (3N\omega_{\text{r}}^2\omega_{\text{z}})^{1/3}$ and the ground-state energy of condensed bosons is $E_{\text{G}} = \hbar\omega_{\text{r}} + (\hbar\omega_{\text{z}}/2)$. For the dipole trap and $N = 2.5 \times 10^5$ [18], the ratio $V_{\text{a}}/V_{\text{b}} = (E_{\text{F}}/E_{\text{G}})^{3/2} = 102$. With $a_{\text{bg}} = 174a_{\text{B}}$, $\mu_{\text{co}} \sim 2\mu_{\text{B}}$, and the mean density $n = 2 \times 10^{12} \text{ cm}^{-3}$, we obtain $\chi = 0.19$, which is less than the threshold $\chi_{\text{c}} = \sqrt{2}/4$. Therefore, ${}^{40}\text{K}$ atom pairs can be completely converted to bosonic molecules in the adiabatic limit. Indeed, a conversion efficiency of up to 90% has been observed [18].

For ${}^6\text{Li}$, with equations (17) and (18) we have also calculated numerically the conversion efficiency as a function of sweeping rates. Comparison between our theory and the experimental

⁷ The cutoff k_{c} is chosen such that the tunnelling window $2\delta_{\text{c}}$ for converting atomic fermions to molecular bosons is consistent with the Feshbach resonance width $\mu_{\text{co}}\Delta B$ of ${}^6\text{Li}$.

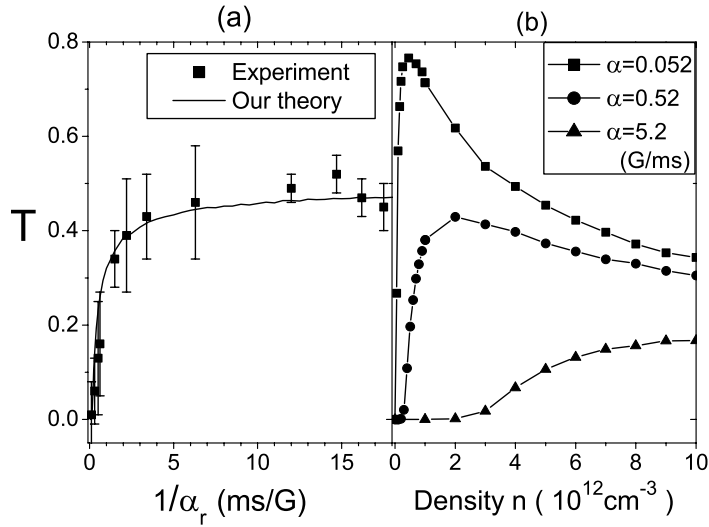


Figure 4. (a) Comparison between our theory and the experimental data of ${}^6\text{Li}$ [11] for the conversion efficiency T as a function of field sweep rates. (b) The dependence of T on the mean atomic density.

data is shown in figure 4(a). They are in good agreement. In addition, our model predicts a non-monotonic dependence of the conversion rate on the mean atomic density (see figure 4(b)). This can be understood with equations (21) and (22). In equation (21), we see that the effective sweeping rate α is inversely proportional to the atomic density. So, increasing the density will reduce the effective sweeping rate and therefore enhance the conversion rate. On the other hand, higher density means larger nonlinearity χ as indicated in equation (22), which in turn suppresses the atom–molecule conversion. These two factors compete with each other, giving rise to the non-monotonic curves in figure 4(b). Therefore, to design experiments of high conversion efficiencies, one needs to carefully choose the initial fermionic atom density so that it falls into the optimal parameter regime.

The relation between the background scattering lengths used in the above discussion is derived in the zero-range approximation and may be corrected due to the finite range of interatomic potential. This correction can modify the factor of 2.3 appearing in the nonlinear parameter in equation (26). The correction is estimated to be of the order of r_0/a_{bg} , where r_0 is the potential range. For example, for the dimer–dimer interaction a_{bb} , the factor of 0.6 is corrected by approximately $0.24(r_0/a_{\text{bg}})$ [36]. The range r_0 is given by $r_0 = \frac{1}{\sqrt{8}} \frac{\Gamma(3/4)}{\Gamma(5/4)} \left(\frac{mC_6}{\hbar^2} \right)^{1/4}$ [37]. For ${}^6\text{Li}$, we have $r_0/a_{\text{bg}} = 0.5$. So, the correction to the factor of 2.3 in the nonlinear parameter is about 20%. For ${}^{40}\text{K}$, $r_0/a_{\text{bg}} = 0.3$ and the high-order correction to the factor of 2.3 is about 12%.

4. Discussion and conclusion

The Feshbach conversion of fermionic atoms into bosonic molecules in a sweeping magnetic field that crosses a resonance is currently a topic of great interest and is under intense investigation both theoretically and in experiments. The molecule formation process has been

widely studied based on a variety of classical and quantum models. The existing theories include the LZ model of two-body molecular production [13, 14] and its many-body extension at zero temperature [15]–[17], the classical phase-space density model [18], and the equilibrium isentropic model at finite temperatures [19]. However, there is still inconsistency between the theories and experimental data. For example, the LZ-type theories [13]–[17] predict a 100% molecular conversion for sufficiently slow sweeps, which is obviously overoptimistic compared with experimental observation [10]–[12]. And the theories [38, 39], which consider only one potential partner for each atom and give a ceiling of 50% for the fermionic conversion [38, 39], are found to be inconsistent with more recent data [18]. The classical equilibrium isentropic model [19] has covered almost all existing experimental data including those in [18], but it finds the data of the Rice experiment [11] far below its prediction. Note that the uniqueness of the Rice experiment compared with all others is its very narrow Feshbach resonance.

Our present work has discussed the role of the interactions between particles in the Feshbach conversion of fermionic atom pairs into molecular bosons, which is ignored in previous quantum models. We show that for the narrow Feshbach resonance the role of particles is significant and can lead to a ceiling of less than 100% on the conversion efficiency. Our main point is that, in the Feshbach conversion process, the molecular conversion efficiency is suppressed by the particle interactions, which serve as an effective internal field appended to the uniform external sweeping magnetic field. The magnitude of this effect is determined by the ratio between the particle-interaction strength and the Feshbach resonance width. In the Rice experiment, the resonance is very narrow so that the conversion efficiency can be dramatically suppressed by the particle interactions. Our theory is consistent with existing experiments. Our model also predicts a non-monotonic dependence of the conversion rate on the mean atomic density, which is important for the optimal choice of parameters in future Feshbach experiments.

Acknowledgments

This work was supported by the NSF of China (10725521, 10604009 and 10504040) and the 973 Project (2006CB921400 and 2007CB814800). BW is also supported by the ‘BaiRen’ programme of the Chinese Academy of Sciences.

References

- [1] Timmermans E, Tommasini P, Hussein M and Kerman A 1999 *Phys. Rep.* **315** 199
- [2] Duine R A and Stoof H T C 2004 *Phys. Rep.* **396** 115
- [3] Chen Q, Stajic J, Tan S N and Levin K 2005 *Phys. Rep.* **412** 1
- [4] Köhler T, Góral K and Julienne P S 2006 *Rev. Mod. Phys.* **78** 1311
- [5] Inouye S, Andrews M R, Stenger J, Miesner H-J, Stamper-Kurn D M and Ketterle W 1998 *Nature* **392** 151
- [6] Timmermans E, Furuya K, Milonni P W and Kerman A K 2001 *Phys. Lett. A* **285** 228
Holland M, Kokkelmans S J J M F, Chiofalo M L and Walser R 2001 *Phys. Rev. Lett.* **87** 120406
Ohashi Y and Griffin A 2002 *Phys. Rev. Lett.* **89** 130402
- [7] Regal C A, Greiner M and Jin D S 2004 *Phys. Rev. Lett.* **92** 040403
- [8] Bartenstein M, Altmeyer A, Riedl S, Jochim S, Chin C, Hecker Denschlag J and Grimm R 2004 *Phys. Rev. Lett.* **92** 120401
- [9] Zwierlein M W, Stan C A, Schunck C H, Raupach S M, Kerman A J and Ketterle W 2004 *Phys. Rev. Lett.* **92** 120403
- [10] Regal C A, Ticknor C, Bohn J L and Jin D S 2003 *Nature* **424** 47

- [11] Strecker K E, Partridge G B and Hulet R G 2003 *Phys. Rev. Lett.* **91** 080406
- [12] Cubizolles J, Bourdel T, Kokkelmans S J J M F, Shlyapnikov G V and Salomon C 2003 *Phys. Rev. Lett.* **91** 240401
- [13] Zener C 1932 *Proc. R. Soc. A* **137** 696
Landau L D and Lifshitz E M 1977 *Quantum Mechanics* (Oxford: Pergamon)
- [14] Góral K, Köhler T, Gardiner S A, Tiesinga E and Julienne P S 2004 *J. Phys. B: At. Mol. Opt. Phys.* **37** 3457
- [15] Pazy E, Tikhonenkov I, Band Y B, Fleischhauer M and Vardi A 2005 *Phys. Rev. Lett.* **95** 170403
- [16] Tikhonenkov I, Pazy E, Band Y B, Fleischhauer M and Vardi A 2006 *Phys. Rev. A* **73** 043605
- [17] Altman E and Vishwanath A 2005 *Phys. Rev. Lett.* **95** 110404
- [18] Hodby E, Thompson S T, Regal C A, Greiner M, Wilson A C, Jin D S, Cornell E A and Wieman C E 2005 *Phys. Rev. Lett.* **94** 120402
- [19] Williams J E, Nygaard N and Clark C W 2004 *New J. Phys.* **6** 123
Williams J E, Nygaard N and Clark C W 2006 *New J. Phys.* **8** 150
Watabe S and Nikuni T 2008 *Phys. Rev. A* **77** 013616
- [20] Javanainen J, Koštrun M, Zheng Y, Carmichael A, Shrestha U, Meinel P J, Mackie M, Dannenberg O and Suominen K A 2004 *Phys. Rev. Lett.* **92** 200402
- [21] Wu B and Niu Q 2000 *Phys. Rev. A* **61** 023402
- [22] Liu J, Fu L, Ou B-Y, Chen S-G, Choi D, Wu B and Niu Q 2002 *Phys. Rev. A* **66** 023404
- [23] Barankov R A and Levitov L S 2004 *Phys. Rev. Lett.* **93** 130403
Andreev A V, Gurarie V and Radzihovsky L 2004 *Phys. Rev. Lett.* **93** 130402
Dukelsky J, Dussel G G, Esebbag C and Pittel S 2004 *Phys. Rev. Lett.* **93** 050403
- [24] Miyakawa T and Meystre P 2005 *Phys. Rev. A* **71** 033624
- [25] Yi W and Duan L-M 2006 *Phys. Rev. A* **73** 063607
- [26] Kokkelmans S J J M F, Milstein J N, Chiofalo M L, Walser R and Holland M J 2002 *Phys. Rev. A* **65** 053617
- [27] Chen Q and Levin K 2005 *Phys. Rev. Lett.* **95** 260406
- [28] Truscott A G, Strecker K E, McAlexander W I, Partridge G B and Hulet R G 2001 *Science* **291** 2570
Hulet R G, Strecker K E, Truscott A G and Partridge G B 2002 *Laser Spectroscopy: Proc. XV Int. Conf.* (Singapore: World Scientific)
Regal C A, Greiner M and Jin D S 2004 *Phys. Rev. Lett.* **92** 040403
- [29] Diener R B and Ho T-L 2004 arXiv:cond-mat/0405174
- [30] Anglin J R and Vardi A 2001 *Phys. Rev. A* **64** 013605
- [31] Yaffe L G 1982 *Rev. Mod. Phys.* **54** 407
- [32] Landau L D and Lifshitz E M 1977 *Mechanics* (Oxford: Pergamon)
- [33] Liu J, Wu B and Niu Q 2003 *Phys. Rev. Lett.* **90** 170404
- [34] Skornyyakov G and Ter-Martirosian K A 1956 *Zh. Eksp. Teor. Fiz.* **31** 775
Skornyyakov G and Ter-Martirosian K A 1957 *Sov. Phys.—JETP* **4** 648
Petrov D S, Salomon C and Shlyapnikov G V 2004 *Phys. Rev. Lett.* **93** 090404
- [35] Jensen L M, Makela H and Pethick C J 2007 *Phys. Rev. A* **75** 033606
Pethick C J 2008 Private communication
- [36] Petrov D 2008 Private communication
- [37] Gribakin G F and Flambaum V V 1993 *Phys. Rev. A* **48** 546–53
- [38] Pazy E, Vardi A and Band Y B 2004 *Phys. Rev. Lett.* **93** 120409
- [39] Chwedeńczuk J, Góral K, Köhler T and Julienne P S 2004 *Phys. Rev. Lett.* **93** 260403